

The relationship between Soliton and Seismic Wave and the center of 2011 TOHOKU Great Earthquake.(Science of form)

\*Masaru Nishizawa<sup>1</sup>

1.none

1. Preface : We had feelled two strong earthquake north of Fukusima Prefecture in the earthquake of 2011 the TOHOKU District Pacific Ocean Earthquake.

In this paper, in this second strong earthquake, the soliton was occurred. (Fig.-1) Still more the second strong earthquake was occurred along the axis of the Japan trench. I could proved two methods.

2. The relationship between Soliton and the center of this earthquake.

At K-NET Oshika (MYG011)(Fig.-1), the epicenter length is 121km. This center is first earthquake motion in seismic wave.

Depend on reference (2), Slip Progression in terms of ship amount is spreading off the coast of MIYAGI Prefecture and is spreading to the north part direction along the axis of the Japan trench after 50 seconds. After 60 secs~100secs, large slip is spreading off the coast from the southern part IWATE prefecture to the north part of FUKUSHIMA prefecture along the axis of the Japan trench. (Fig-4 in reference (2))

In this reference, the total moment rate function (fig-5 in reference (2)) showes Soliton. It is as clear as day. (refer to Fig.-1)

This peak point happened before and after the 80 sec of Seismic moment rate. Therefore this reference showes the second earthquake motion along the axis of the Japan trench.

3. Relationship between Soliton and still more location of the second strong earthquake motion and Seismic Wave.

At K-NET Tsukidate (YYG004) or K-NET Oshika (MYG011), strong-motion accelerograms continues for two earthquake motions in Seismic Wave. In short, the first seismic wave peak and the second seismic wave peak quaked continuous motion. Two strong motion with a small continuous shocks of an earthquake in between exist. For that reason, the second earthquake motion had happened off the coast of the first earthquake motion.

Abstract

1. Strong-motion accelerograms recorded at K-NET Tsukidate (MYG004) or Oshika (MYG011 and others) express clearly a continuation of two earthquake motion.

Therefore the second earthquake motion had happened off the coast of the first earthquake motion. And still more the second earthquake motion was occurred along the axis of the Japan trench. It is an earthquake directly above its epicenter. That's perfectly right.

2. the total moment rate function (Fig.-5 in reference (2)) shows Soliton.

Reference

1) Sekiguchi, H., Irikura, K., and Iwata, T. (2000): Fault geometry at the rupture termination of the 1995 Hyogo-ken Nanbu earthquake. Bull. Seismol. Soc. Am., 90-1, 117-133, doi:

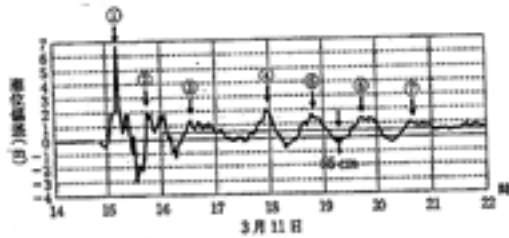
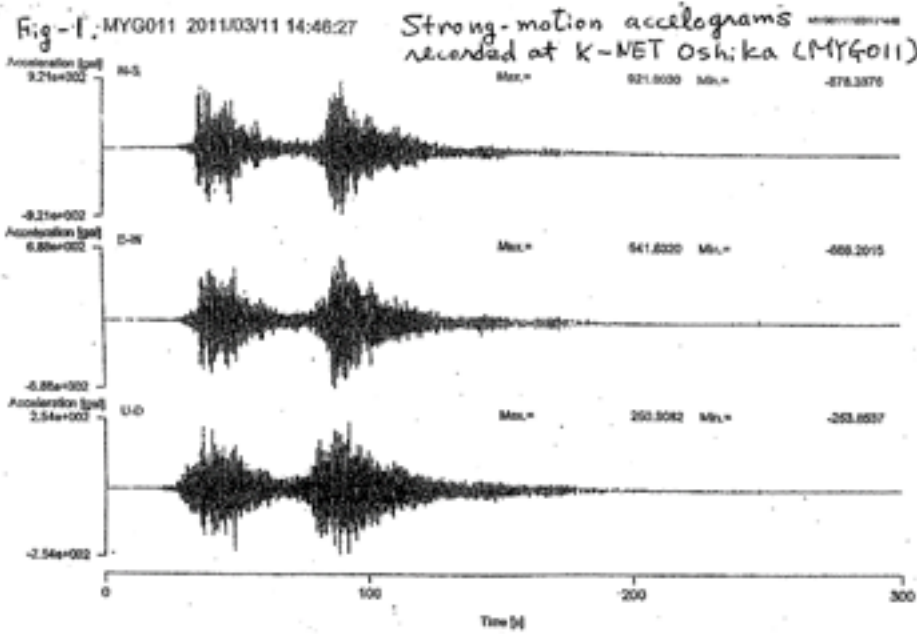
10.1785/0119990027

2) Wataru SUZUKI, Shin AOI, Haruko SEKIGUCHI, and Takashi KUNUGI. (2012): Source Rupture Process of the 2011 off the Pacific Coast of Tohoku Earthquake Derived from Strong-Motion Records. Bull. Research Report on the 2011 Great East Japan Earthquake Disaster.: March 2012, Natural Disaster Report No. 48: National Research Institute for Earth Science and Disaster Prevention, Japan.

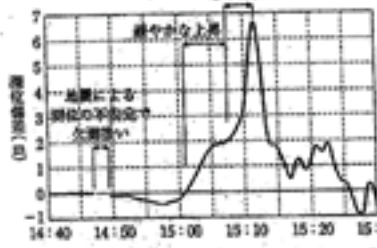
3) Masaru Nishizawa. (2013): The Relationship between in GPS wave gage and Seismic Wave of 2011 the Tohoku District Pacific Ocean Earthquake.: May 19-24 2013 JpGU

Keywords: 2011 the TOHOKU District pacific Ocean Earthquake, Two strong earthquake motion, Soliton, Total moment rate, Science of Form

防災科学技術研究所主要災害調査 第48号 2012年3月



Soliton ① is recognized in GPS Wave gage of 2011 the Tohoku District Pacific.



Written by Kozuo Oike, "Great Earthquake of The Japan Islands", Iwanami Science Library, -185, P10.

尾池和夫著「日本列島の巨大地震」岩波科学ライブラリ-185, P10.

① + Soliton ② ~ ⑦: Break down of Solitary <sup>Wave</sup> Solitons.

Reference "Hydrodynamics", Written by Mikio Hino, Asakura publisher, 1992

参考: 日野幹雄著「流体力学」朝倉書店, 1992

## Design and Implementation of the National Seismic Monitoring Network in the Kingdom of Bhutan

\*Shiro Ohmi<sup>1</sup>, Hiroshi Inoue<sup>2</sup>, Jamyang Chopel<sup>3</sup>, Kinley Namgay<sup>3</sup>, Dowchu Drukpa<sup>3</sup>

1.Earthquake Hazards Division, Disaster Prevention Research Institute, Kyoto University, 2.National Research Institute for Earth Science and Disaster Prevention , 3.Department of Geology and Mines, Ministry of Economic Affairs, Kingdom of Bhutan

Bhutan-Himalayan district is located along the plate collision zone between Indian and Eurasian plates, which is one of the most seismically active region in the world. Recent earthquakes such as M7.8 Nepal earthquake in April 25, 2015 and M6.7 Imphal, India earthquake in January 3, 2016 are examples of felt earthquakes in Bhutan. However, there is no seismic monitoring system established in Bhutan, whose territory is in the center of the Bhutan-Himalayan region.

In this project, we are establishing the first national permanent seismic monitoring network in the Kingdom of Bhutan that is utilized for not only for seismic disaster mitigation of the country but also for studying the seismotectonics in the Bhutan-Himalayan region which is not precisely revealed due to the lack of observation data in the past.

We started establishing permanent seismic monitoring network of minimum requirements which is composed of six (6) observation stations in Bhutan with short period high sensitivity and strong motion seismometers as well as three (3) broad-band seismometers. Obtained data are transmitted to the central processing computers in the DGM (Department of Geology and Mines, Ministry of Economic Affairs) office in Thimphu. In this project, DGM will construct seismic vault with their own budget which is approved as the World Bank project and Japan team assists the DGM for site survey of candidate observation site, designing the observation vault, and designing the data telemetry system as well as providing instruments for the observation such as seismometers and data recorders.

We already started the operation of the first telemetry seismic station located in Thimphu city, the capital in western Bhutan, and will soon start operation in Bumthang district, central Bhutan. Continuous seismic record from Thimphu station is already stored in the data center in DGM. We also deployed two offline seismic stations with short period seismometers in Gasa (Northern Bhutan) and Wangdu (Central) to assist permanent seismic network.

Keywords: Bhutan-Himalayan district, Seismic Observation Network

## An improvement of JMA's earthquake catalog

\*Satoshi Takahama<sup>1</sup>, Koji Tamaribuchi<sup>1</sup>, Ken Moriwaki<sup>1</sup>, Kana Akiyama<sup>1</sup>, Nobuyuki Hirota<sup>1</sup>, Naoyuki Yamada<sup>1</sup>, Masaki Nakamura<sup>1</sup>, Tetsuo Hashimoto<sup>1</sup>

### 1. Japan Meteorological Agency

Based on the policy of the Headquarters for Earthquake Research Promotion, Japan Meteorological Agency(JMA) collects the data of the high-sensitive seismographs nationwide, performs the processing of hypocenter determination centrally, and publishes the result as the earthquake catalog.

In the current earthquake catalog, we list earthquakes that are limited by a certain criteria as a result of scrutiny. After the 2011 off the Pacific coast of Tohoku Earthquake, although aftershocks have decreased, seismic activity is located in the active situation in comparison with the previous. So we are processing them to raise the lower limit of the magnitude of earthquakes to be processed. Therefore, there is an earthquake smaller than the processing limit that is not listed in the earthquake catalog even if detected by automatic processing.

Against the background of this thing, under the Earthquake Research Committee, an examination for improvement for the way of earthquake catalog was performed in 2013 fiscal year, and summarized reports that shows three directions, 1) to maintain the earthquake detection capability, 2) to list all of the earthquakes detected to the earthquake catalog, 3) to perform the quality management with a stage to accuracy.

Based on this report, JMA is planning to improve and change the hypocenter determination process, utilizing automatic hypocenter etc. In the next catalog, we will promote efficiency of the work procedure as follows.

We utilize the automatic hypocenters in case of the earthquakes smaller than the limit of the magnitude based on the area and the depth of the hypocenter, and we list the earthquakes almost uniformly scrutinized by hands as before in case of the earthquakes larger than this limit. And if the automatic hypocenter is not determined, we list the earthquakes by hands with the simple method using the data of the max about 10 seismic stations.

The lower limit of the scrutinized earthquakes is about M2 in case of shallow and inland earthquakes. This lower limit increases with distances from the coast of the lands, and the max lower limit is about M4.

And newly we introduce registration flags indicating the difference in processing method and the accuracy of the hypocenter.

Here, we will give the concrete examples of materials JMA made with the new earthquake catalog, such as the seismicity map.

Keywords: earthquake catalog

## Compiling the source area data of large earthquakes in the world

\*Yuzo Ishikawa<sup>1</sup>

1.The National Institute of Advanced Industrial Science and Technology

The earthquake sources in the world are estimated by the area obtained by the one month aftershock distributions. Most of events of which magnitude are larger than 7.5 from 1970, using mainly PDE earthquake catalog. Some large events in 20 century were added using the intensity distributions.

Keywords: source area, large earthquake

The difference between JMA magnitude and moment magnitude in terms of seismic efficiency

\*Kiyohiko Yamamoto

1. Introduction: For large earthquakes occurring along the Japan trench except for the off Miyagi Pref. region, moment magnitude  $M_w$  is 0.4 larger than the JMA magnitude  $M_j$ . Here,  $M_j$  and  $M_w$  are proportional to logarithms of seismic energy  $E_s$  and released moment  $M_o$ , respectively.  $M_o$  is proportional to the relative displacement  $u_b$  of fault surfaces.  $E_s$  depends on directly seismic efficiency  $f$ , but  $M_o$  does indirectly. Thus the difference is thought to reflect the degree of the dependence on  $f$ .

$f$  is a function of the rupture velocity  $V_r$  and is large for a large  $V_r$ . The small  $M_j$  compared with  $M_w$  thus suggests the small  $V_r$ . The difference between  $M_j$  and  $M_w$  is discussed from this viewpoint for The Tohoku earthquake (2011/3/11,  $M_w$ 9) as an example.

2.Theory: The damage zone fault model of earthquakes\* is employed for the present discussion. In this model, a fault zone with a uniform thickness constitutes of damaged rock area and asperity area. Fault surfaces mean the boundaries between fault zone and host rock blocks. The damaged rocks have relaxed during a long time after the preceding faulting. An asperity has the same elastic constants as the host rocks. Faulting occurs at the time that the relative displacement  $u_b$  reaches the critical value.

For faulting, energy balance is written by

$$P_a + P_b = E_s + W, \quad E_s = f \times P_b. \quad (1)$$

Here,  $P_a$  and  $P_b$  respectively are strain energies in the asperity and in the host rock blocks.  $P_b$  is approximated by the strain energy released when a circular crack is produced in a homogeneous host rocks under the uniform stress, that is equal in magnitude to the average stress drop due to faulting.

$W$  is apparent fracture energy that is equivalent to the work to the host rocks done by the vertical displacement of the fault surfaces. The displacement is produced by the rotation of damaged rocks accompanied by the rupture propagation in a fault zone.

A linear relation has been found between the width of fault damage zone and the length of fault (Vermilye, J. M., and C. H. Scholz, 1998). In order to link the model to fault size, the linear relation is adopted.\* Further, Sato and Hirasawa (1973) present an approximate relationship between  $V_r$  and  $f$  for a circular crack. This relationship is used for the present discussion.

3. Results: For  $f=1$ , all strain energy  $P_b$  is dissipated as  $E_s$ . The fraction of asperity area is about 2% of the fault zone area.  $V_r$  is approximately equal to the S-wave velocity of host rocks. For  $f$  close to zero, all strain energy  $P_a + P_b$  is used for the rupture propagation and  $E_s$  and  $V_r$  go to zeros. These may be the characteristics of so-called slow slip events. The fraction tends to about 0.74%. This is 0.37 times of the fraction at  $f=1$ . This means that the displacement and the average stress drop decrease to 0.37 times of those at  $f=1$ .

The relationships between  $E_s$  and  $M_j$  and between  $M_o$  and  $M_w$  respectively are written by

$$\log E_s = 1.5M_j + 4.8 \quad (2)$$

$$\log M_o = 1.5M_w + 9.1. \quad (3)$$

For a constant fault area, Eq. (2) and Eq. (3) intersect around  $f = 0.8$ . This suggests that the seismic efficiency is about 0.8 for majority of earthquakes. For  $f = 0.8$ ,  $V_r$  is determined at about 0.8 times of S-wave velocity  $V_s$  of host rock.

Referring to the report by JMA\*\*,  $M_j$  and  $M_w$  of The Tohoku earthquake are 8.4 and 9.0, respectively, and  $V_r$  and  $V_s$  are about 1.8km/s and about 3.4 km/s, respectively.  $V_r$  is about 0.53 times of  $V_s$ . From the relationship of  $V_r$  and  $f$ ,  $f$  is estimated at about 0.3.  $M_j$  is estimated at about 8.6 for  $f$

= 0.3 and  $M_w=9.0$ . The estimated  $M_j$  tends to the observed one. This suggests that the small  $M_j$  is due to the small  $V_r$ .

Note: \*Yamamoto and Yabe, 2009; <http://kynmt.in.coocan.jp/> ;(REFERENCE/23)

\*\*<http://www.jma.go.jp/jma/kishou/books/gizyutu/133/ALL.pdf>

Keywords: Seismic efficiency, Moment magnitude, JMA magnitude, Slow slip event, Rupture velocity, Damagezone fault model of earthquake

## Long-term seismic quiescence before the 2010 $M_w$ 8.8 Chile earthquake and the 2001 $M_w$ 8.4 Peru earthquake

\*Kei Katsumata<sup>1</sup>

1. Institute of Seismology and Volcanology, Hokkaido University

An earthquake catalog created by International Seismological Center (ISC) was analyzed in the study area, 65°W to 80°W, 10°S to 60°S, between 1 January 1964 and 31 December 2009, including 1062 earthquakes shallower than 60 km with the body wave magnitude of 5.0 or larger. Clustered events such as earthquake swarms and aftershocks were removed from the ISC catalog by using a stochastic declustering method developed by Zhuang et al. (2002). A detailed analysis of the earthquake catalog using a gridding technique (ZMAP) shows that the seismic quiescence areas are found in and around the focal area of the 2010  $M_w$ 8.8 Chile and the 2001  $M_w$ 8.4 Peru earthquakes. The seismic quiescence area for the 2010 Chile earthquake is a circle centered at (36.7°S, 73.1°W) with a radius of 144 km. The seismicity rates in this area are 1.1 events/year between 1964.0 and 1990.4, 0.19 events/year between 1990.4 and 2004.3, and 0.83 events/year between 2004.3 and 2010.0. The seismic quiescence area for the 2001 Peru earthquake is a circle centered at (17.7°S, 72.1°W) with a radius of 113 km. The seismicity rates in this area are 0.76 events/year between 1964.0 and 1990.4 and 0.0 events/year between 1990.4 and 2000.5. In the case of the Chile earthquake the seismic quiescence ended six years before the main shock on 27 February 2010. On the other hand, in the case of the Peru earthquake the seismic quiescence ended at the almost same time as occurrence of the main shock on 23 June 2001.

Keywords: seismic quiescence, ZMAP, the 2011 Chile earthquake, the 2001 Peru earthquake



## Influence of the 2011 Tohoku, Japan earthquake on the Korean peninsula

\*Sun-Cheon Park<sup>1</sup>, Jun-Whan Lee<sup>1</sup>, Hyojin Yang<sup>1</sup>, Eun Hee Park<sup>1</sup>, Won-Jin Lee<sup>1</sup>

1.National Institute of Meteorological Research, Korea Meteorological Administration

The 2011 Tohoku, Japan earthquake (M9.0) not only produced catastrophic damage in Japan but influenced on the Korean peninsula in terms of the seismicity, tsunami and crustal deformation. Seismic waves were large enough to be saturated in broadband seismic stations equipped with STS-2 seismometer which were located in the eastern part of the peninsula. Also small tsunami waves were observed along the southern and eastern coast. We have analyzed the tsunami as well as the seismic activity and crustal movement to understand the influence of the Tohoku earthquake on the Korean peninsula which is located about 10~15 degrees far from the fault plane.

Tsunami generated by the Tohoku earthquake propagated to the Korean peninsula as well. Tsunami with the height of less than 30 cm was observed about 3~5 hours later at the water level stations in southern and eastern coast of the peninsula, as can be expected by numerical tsunami simulation. However, some water level changes occurred even a few minutes after the earthquake at the several water level stations in north-eastern part of South Korea. We calculated horizontal displacements as well as vertical ones in the surrounding seas of the peninsula using the slip distribution obtained by the seismic waveform inversion (Baag et al., submitted). Then the tsunami was calculated considering the bathymetry effect or the effect of the horizontal displacement and the seafloor slope, following Murotani et al. (2015). As the result, the unexpected tsunami observed a few minutes later seems to have a coincidence with the tsunami generated by the bathymetry effect. The level of seismicity was changed by the Tohoku earthquake. Even though only three earthquakes with magnitude greater than 2 were reported by the Korea Meteorological Administration (KMA) within 5 days since the event, 53 events including micro earthquakes were identified using continuous waveforms only in the day of the earthquake (Park, 2012). Unusually large increase of seismic events was observed rather in 2013. Those events include three moderate earthquakes of M~5 and intensive swarm in the Yellow Sea region. Hong et al. (2015) interpreted that this phenomenon was induced by the fluid diffusion during the transient tension field and pore pressure increase during the ambient compressional-stress field recovery.

Crustal deformation was determined using the GNSS data densely distributed in the Korean peninsula. The displacements induced by the earthquake were about 1.5~4 cm. The crust moved toward the direction of the fault, which was to the east and it differs from the general movement of this region before the Tohoku earthquake. And the trend of eastward movement continued at least until 2012. The annual velocity of crustal deformation showed that the movement was recovered to the general direction since 2013.

These analyses indicate that the Tohoku earthquake has directly influenced on the Korean peninsula. And it may be necessary to consider the influence of another large earthquake that can be expected around the Japanese islands, like expected Nankai earthquake.

Keywords: 2011 Tohoku, Japan earthquake, tsunami, crustal deformation, seismicity, Korean peninsula

## Analysis of foreshock sequence of the 2014 $M_w$ 6.2 Northern Nagano earthquake: Implications for slow-slip transient and unusual source property

\*Kazutoshi Imanishi<sup>1</sup>, Takahiko Uchide<sup>1</sup>

1.Geological Survey of Japan, AIST

The  $M_w$  6.2 Northern Nagano earthquake occurred on November 22, 2014, central Japan, which broke a northern part of the Itoigawa-Shizuoka Tectonic Line active fault system. The earthquake has a foreshock sequence from four days before the mainshock, which was captured by a dense permanent seismic observation. We first determined hypocenters of foreshocks, mainshock, and aftershocks by assuming two different one-dimensional velocity models to account for heterogeneous structure in the area. We then applied the double-difference (DD) method to improve the precision of event relative locations. The DD location reveals that the foreshocks were located at a depth of 3-4 km and distributed on a NNW dipping 1 km x 1 km plane with an angle of about 60 degree (plane A), which is distinct from the aftershock distribution. The geometry of the plane A is consistent with the foreshock focal mechanisms determined by P-wave polarities as well as body-wave amplitudes. We also found that the foreshock sequence is located at the eastern extension of two Neogene faults described in the geological sheet map at 1:50,000 (Geological Survey of Japan, 2002), where the strike of one of the faults agrees well with that of the plane A. These Neogene faults cut active folds as well as Otari-Nakayama fault, making the region become a local structural heterogeneity. We infer that the foreshock sequence appears associated with fault zone complexity, as suggested for other foreshock sequences (e.g., Chen and Shearer, 2013).

In order to investigate the foreshock sequence in more detail, we analyzed seismograms recorded at Hakuba Hi-net station, which is a 632-m deep borehole station located about 5 km west of the foreshock region. By a visual identification of running spectra at the Hakuba station and S-P time, we newly detected 384 foreshocks, which are nearly seven times more than those in the JMA catalogue. We determined their locations and magnitudes on the basis of waveform cross-correlations and amplitude ratios, respectively, between newly detected foreshocks and DD relocated events. Our new catalogue delineated another plane with a N-S striking vertical plane (plane B), which is consistent with one of nodal planes of the P-wave first-motion mechanism of the mainshock. The spatial and temporal distribution of our new catalogue indicates that the foreshock sequence started at the deeper part of the plane A, migrating to the shallower part, and then jumped to the plane B, migrating to the mainshock hypocenter. The migrating speed is less than a few km/day, implying a possible slow-slip transient. A hypothesis is that the foreshock sequence is driven by aseismic slip, which causes stress loading at the mainshock hypocenter and triggers the mainshock. We further determined source parameters of the foreshocks to investigate their fault properties. We applied Multi-Window-Spectral-Ratio method (Imanishi and Ellsworth, 2006) to the foreshocks and aftershocks using the deep borehole data. The estimated corner frequencies of aftershocks decrease with magnitude and indicate constant stress drop. In contrast, the estimated corner frequencies of foreshocks are almost constant over nearly two orders of magnitude. The constant corner frequency suggests that fault dimension is the same regardless of magnitude or stress drop increases with magnitude under an assumption of scale-invariant rupture velocity. It is noted that the same observation was reported for the foreshock sequence of the 1999  $M_w$ 7.6 Izmit earthquake, Turkey (Bouchon et al., 2011), which may indicate that the constant corner frequency or the size-dependent stress drop is a common specific property of foreshocks.

Acknowledgements: Seismograph stations used in this study include permanent stations operated by NIED Hi-net, JMA, ERI, and DPRI.

Keywords: 2014 Northern Nagano earthquake, foreshock, source property, slow slip

Delayed triggering process of the  $M_{JMA}6.4$  Eastern Shizuoka earthquake on March 15, 2011 by analyses of stress changes and detection of foreshocks

Rina Tamura<sup>1</sup>, \*Masatoshi Miyazawa<sup>2</sup>

1.Graduate School of Science, Kyoto University, 2.Disaster Prevention Research Institute, Kyoto University

We investigated the triggering process of the  $M_j6.4$  Eastern Shizuoka earthquake on March 15, 2011, which occurred 4 days after the 2011  $M_w9.0$  Tohoku-Oki earthquake and about 4 minutes after the  $M_j6.2$  Fukushima-Oki earthquake. We obtained a static Coulomb failure stress change on the fault of the Eastern Shizuoka earthquake by the Tohoku-Oki earthquake, which was about 21 kPa, and the largest dynamic stress change by the passing surface waves was about 200 kPa. The largest dynamic Coulomb failure stress change from the Fukushima-Oki earthquake and tidal stress change after the Tohoku-Oki and before the Eastern Shizuoka earthquake were about 0.3 kPa and 1.2 kPa, respectively, while those at the onset of the Eastern Shizuoka earthquake were negative values of about -0.01 kPa and -0.2 kPa. We also tried to detect earthquakes immediately preceding the Eastern Shizuoka earthquake using a matched filter technique and found one  $M1.0$  event that located about 2 km NNE from the mainshock and occurred about 17 hours before it. However, this event may not be identified as a foreshock according to the background seismicity before 2011 in this region. We propose that delayed triggering (clock advance) might have occurred for the Eastern Shizuoka earthquake, where the frictional stress had rapidly built up due to these static, dynamic, and tidal stress changes when the eventual earthquake was ready to occur.

Keywords: Eastern Shizuoka earthquake, Delayed triggering, Coulomb failure stress change, Foreshock

## Re-analysis of Seismic Quiescence and Slow Slip in Hamanako region

\*Sumio Yoshikawa<sup>1</sup>, Naoki Hayashimoto<sup>1</sup>, Tamotsu Aketagawa<sup>2</sup>

1.Meteorological Research Institute, 2.Okinawa Regional Headquarters

We have shown a remarkable spatial correlation between the seismic quiescence in the Philippine Sea plate and the Long-term Slow Slip Event (LSSE) in the plate boundary beneath Hamanako region, though did not have shown a clear time correlation between them (SSJ, 2015). Against this, according to JMA (since September 2014), the seismicity in the crust of the central western Shizuoka becomes low simultaneously with two times of LSSE in the plate boundary beneath Hamanako region, which suggests a clear time correlation between the seismic quiescence and LSSE. On the other hand, Kobayashi and Yoshida (2004) and Yamamoto et al. (2005) have pointed out occurrence of LSSE in the period from 1988 to 1990. If LSSE are repeating similarly in this region, it is important to clarify how LSSE can be caused at the same time when the quiescence in the crust of the central western Shizuoka appears, and to make clear the reason why we cannot observe a clear time correlation between the seismicity and LSSE beneath Hamanako region.

We used the eMAP technique (Aketagawa and Ito, 2008; Hayashimoto and Aketagawa, 2010) for space time analyses of seismic quiescence and activation. The attached figure shows source distribution maps of seismic quiescence and activation detected by the eMAP for the earthquakes with the magnitude equal to and larger than 1.1 in the central western Shizuoka and around Hamanako. The epicenter map (a) shows concentration of quiescence areas near the Suruga bay and around Hamanako. The vertical cross section (b) shows a clear quiescence beneath Hamanako region and activation zones beneath the central western Shizuoka both in the crust and the plate. The activation seems to reflect the seismic activity in a part of the locked zone of the plate boundary inferred by Matsumura (1997). The space time plot (c) shows activation in the SE part continues from 2006 to 2012, whereas it becomes relatively low in the periods from 2001 to 2005 and from 2013 to present, at the same time when LSSE is observed, which supports correspondence of the low seismicity in central western Shizuoka with LSSE as it was pointed out by JMA. Against this, quiescence around Hamanako region is not clearly correspondent with LSSE, though the area of quiescence seems inferior for the rest of LSSE from 2006 to 2012.

We then searched seismic quiescence that previously occurred in the same area from January of 1983 for the earthquakes with the magnitudes equal to and larger than 2.3. As a result of this we confirmed an example also in the period from 1988 to 1990 in a small region of the same area. This result may indicate the possibility that the quiescence in the locked zone occurred with LSSE in the plate boundary beneath Hamanako region as many as three times.

It is possible to explain the mechanism for the correspondence of the quiescence with LSSE if the stress reduction in the locked zone occurs at the same time when LSSE makes stress release in the plate boundary, though it is still complicated to tell the reason why no clear time correlation is found between quiescence and LSSE in the plate beneath Hamanako region. It may be necessary to make more analysis for the seismic activity based on stress distribution caused by heterogeneity within the crust and the plate.

Keywords: Seismic quiescence, Seismic activation, Slow slip event

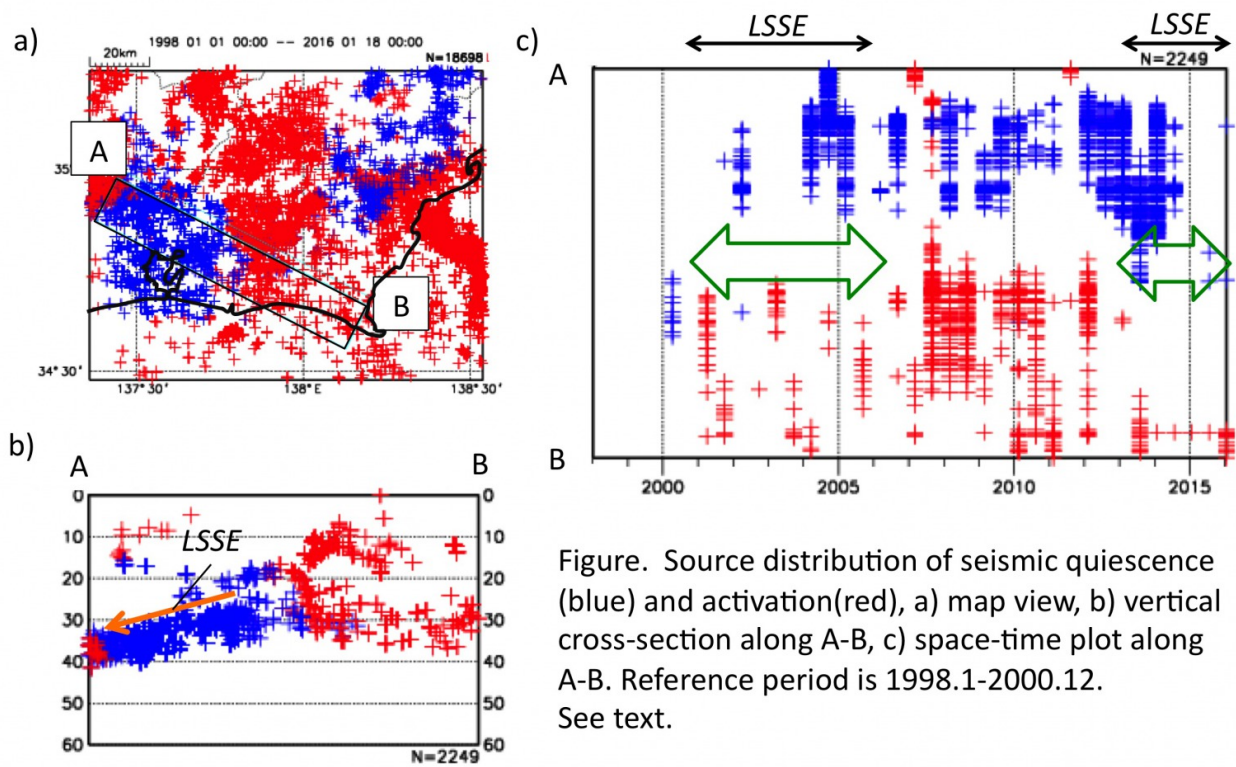


Figure. Source distribution of seismic quiescence (blue) and activation (red), a) map view, b) vertical cross-section along A-B, c) space-time plot along A-B. Reference period is 1998.1-2000.12. See text.

## Temporal change of focal mechanism pattern in the Tohoku-oki region

\*Hiroaki Matsukawa<sup>1</sup>, Yuji Yagi<sup>1</sup>, Bogdan Enescu<sup>1</sup>

1.Geoscience, University of Tsukuba

It is well known that after the occurrence of a megathrust earthquake, a pattern of focal mechanisms of subsequent events changes since stress field near the hypocenter is significantly changed. For example, in the case of the 2011 Tohoku-oki earthquake, the number of normal-fault earthquakes increased after the mainshock (e.g., Asano et al., 2011). Temporal change of the focal mechanism reflects the stress accumulation / release process in-between the megathrust earthquakes and the stress state recovery after the mainshock to pre-mainshock condition. However, there are still few studies discussing the temporal change of focal mechanism at high time resolution. In order to track the temporal change of stress field near the source area of the 2011 Tohoku-oki, we focused on the temporal change of the focal mechanisms in the 2011 Tohoku-oki region.

First, we classified the faulting type of earthquakes in the F-net catalog (National Research Institute for Earth Science and Disaster Prevention) as normal fault, thrust fault and strike-slip fault by following the method of Frohlich (1992). The time window for sampling was fixed to 10 days for after the mainshock and 50 days for before the mainshock. In order to stabilize the temporal change, we defined a sampling sequence so we can include a number of earthquakes more than 500 for after the mainshock and more than 100 for before the mainshock.

The results show that the ratio between the number of normal fault earthquakes to the total earthquakes increases step-wise after the mainshock and gradually decays with time. The gradual decay of the ratio has significant fluctuations and did not reach yet the level before the mainshock. The phenomenon of gradual recovery may reflect the flow of asthenosphere and after slip in deeper area of the hypocenter. It may also reflect changes of stress in the subducting and overriding plate. Moreover, focusing on before the mainshock, we observed the rapid decrease of the ratio. The same phenomenon was not observed from 1997 (start observation by F-net) to before the mainshock. This rapid decrease may relate to the preparation process of the 2011 Tohoku-oki occurrence.

Keywords: focal mechanism pattern, temporal change of focal mechanisms, 2011 Tohoku-oki earthquake

## Sequence of moderate-to-large deep focus earthquakes around Off Ogasawara Islands on 23th June 2015

\*Shunsuke Takemura<sup>1</sup>, Tatsuhiko Saito<sup>1</sup>, Katsuhiko Shiomi<sup>1</sup>

1.National Research Institute for Earth Science and Disaster Prevention

Large deep-focus earthquake with Mw 6.5 occurred around Off Ogasawara (Bonin) Islands, at 21:18 (JST) on 23th June 2015. Observed seismograms of Hi-net, which contain several *P* and *S* waves arrivals during 10 minutes from 21:18 (JST), indicate that relatively large earthquakes sequentially occurred around Japan. In this study, using velocity seismograms of F-net and Hi-net, we investigate seismic wave propagation during sequential earthquakes and estimate the magnitude of each event.

To clarify how seismic waves propagate across Japan during earthquake sequence, we made snapshots of seismic energy propagation by using mean-square (MS) envelopes of Hi-net waveforms. MS envelopes were calculated by sum of three-component filtered seismograms with passed frequency of 1-32 Hz. Then, we took spatial interpolation of amplitudes of MS envelopes at each time step to make smooth spatial distribution of seismic energy at each time step. Snapshots of seismic energy propagation visually show that one earthquake occurred around Sea of Japan and then three earthquakes occurred around Off Ogasawara Islands. Second Off Ogasawara event was not listed in the JMA PDE catalogue. Since the propagation patterns of seismic energy of three earthquakes around Off Ogasawara are very similar, we consider that these earthquakes have similar hypocenter locations. Then, to evaluate magnitude of detected events, we measured maximum *S* wave amplitudes of each earthquake from MS envelopes at F-net station and calculated amplitude ratio with maximum *S* wave amplitude of first earthquake, which has a seismic moment of  $5.47 \times 10^{18}$  Nm (Mw6.5) referred from CMT solution of F-net. Amplitudes ratio and estimated seismic moment are  $0.462 \pm 0.023$  and  $2.52 \pm 0.13 \times 10^{18}$  Nm (Mw6.2 $\pm$ 0.1) for second earthquake, respectively, and  $0.106 \pm 0.004$  and  $5.80 \pm 0.22 \times 10^{17}$  Nm (Mw5.8 $\pm$ 0.1) for third earthquake, respectively.

### Acknowledgement

We use the Preliminary Determined Earthquake catalogue provided by the Japan Meteorological Agency.

Keywords: deep focus earthquake, seismic wave propagation, seismogram envelope, Izu-Bonin arc